Thermochimica Acta 509 (2010) 111–119

Contents lists available at ScienceDirect

Thermochimica Acta

journal homepage: www.elsevier.com/locate/tca

Development of state diagram of bovine gelatin by measuring thermal characteristics using differential scanning calorimetry (DSC) and cooling curve method

Mohammad Shafiur Rahman[a,*], Ghalib Al-Saidi[a], Nejib Guizani[a], Aminah Abdullah[b]

[a] Department of Food Science and Nutrition, College of Agricultural and Marine Sciences, Sultan Qaboos University, P.O. Box-34, Al-Khod-123, Muscat, Oman
[b] Faculty of Science and Technology, Universiti Kebangsaan Malaysia, 43600 UKM Bangi Selangor, Malaysia

ARTICLE INFO

Article history:
Received 17 April 2010
Received in revised form 29 May 2010
Accepted 12 June 2010
Available online 18 June 2010

Keywords:
Glass transition
Freezing point
Un-freezable water
Unfolding temperature
Maximal-freeze-concentration condition
Solids-melting temperature

ABSTRACT

A state diagram of bovine gelatin was developed by measuring the freezing curve, glass transition, unfolding, solids-melting lines, and ultimate maximum-freeze-concentration conditions. The freezing point decreased with the increase of solids; whereas glass transition, unfolding, and solids-melting decreased with the decrease of solids up to solids content 0.84 g/g gelatin and then remained constant. The freezing point, glass transition and solids-melting were modeled by Chen's model based on the Clausius-Clapeyron equation, modified Gordon-Taylor model, and Flory's equation, respectively. The ultimate maximum-freeze-concentration conditions were found as $(T'_m)_u$ equal to −11.9 °C and $(T''_g)_u$ equal to −14.9 °C, and the characteristic solids content, X'_s as 0.80 g/g sample (i.e. un-freezable water, $X'_w = 0.20$), respectively. Similarly the value of T_g^{iv} (i.e. intersection of vertical line passing through T'_m and glass transition line) was estimated as 34 °C.

1. Introduction

Gelatin is a biopolymer that has very broad applications in the food, pharmaceutical and photographic industries. In the food industry gelatin is widely used as a gelling agent. Skin and bone from bovine (beef source) and porcine (pork source) have been usually utilized commercially in gelatin production. In recent years, fish skin gelatin has gained importance as the demand for non-bovine and non-porcine gelatin increased. The quality of a gelatin for a particular application depends largely on its structural functionality, as well as its physico-chemical properties that are greatly influenced not only by the species or tissue from which it is extracted, but also by the severity of the manufacturing method.

Collagen of connective tissue can be hydrolyzed into food grade gelatin used as functional ingredient for different products. Collagen comprises a triple helix structure which forms fibers, arranged in bundles, which are kept together by the connective tissue matrix. When subjected to acid or alkaline hydrolysis, a mild degradation process occurs and the fibrous structure of collagen is broken down irreversibly due to the rupture of covalent bonds. Soluble collagen denatures due to the breakdown of hydrogen and probably electrostatic bonds in hot water (40 °C). This process destroys the triple helical structure of collagen to produce one, two or three random chain gelatin molecules that give a high viscosity solution in water [1].

The physico-chemical properties of gelatin depend on several factors including the method of preparation and intrinsic properties of collagen. In addition to the processing conditions, other factors, such as species, breed, age, manner of feeding the animal, and storage conditions of raw skin also affect the characteristics of extracted gelatin [2]. Obtaining the proper functionality is dependent upon the conformational structure of the protein. It is important to understand thermal characteristics, such as glass transition, freezing point, thermal unfolding, solids-melting, and deterioration of gelatin in order to know its structural characteristics. Glassy materials have been known for centuries but it was only in the 1980s that the technology started to be purposefully applied to foods and a scientific understanding of these systems started to evolve [3]. The early papers concerning glass transition in food and biological systems appeared in the literature in the 1960s [4,5]. Glass transition is a second-order time-temperature dependent transition, which is characterized by a discontinuity or change in the slope of physical, mechanical, electrical, thermal and other properties of a material when plotted as a function of temperature [6–9]. Food materials are in an amorphous or non-crystalline state and below the glass transition temperature materials are rigid

* Corresponding author. Tel.: +968 24141273; fax: +968 24413418.
E-mail address: shafiur@squ.edu.om (M.S. Rahman).

0040-6031/$ – see front matter © 2010 Elsevier B.V. All rights reserved.
doi:10.1016/j.tca.2010.06.011

and brittle. Glasses are not crystalline with a regular structure, but retain the disorder of the liquid state [10]. Physically it is a solid but it more closely resembles a thermodynamic liquid. Duckworth [11] measured solute mobility in relation to water content and water activity and molecular motions are fundamental to the glass transition of polymers [12]. Molecular mobility increases 100-fold above glass transition [9,13–15]. The thermal stability of proteins can be defined as the temperature at which it denatured. An endothermic phenomenon at denatured state was largely attributed to hydrogen bond disruption leading to unfolding of protein [16]. The adsorption of water by dehydrated globular proteins reduced their thermal stability. As moisture content increased, the protein denaturation temperature decreased until reached a plateau, where a further increase in moisture did not promote additional lowering [17]. Solids-melting is usually defined as the temperature when crystalline state of a food material is lost. Freezing point is considered as the temperature when ice is formed in the sample, and it is a first order transition since latent heat is involved.

D'Cruzand and Bell [17] measured the glass transition, thermal unfolding and solids-melting of gelatin as a function of water content for high solids (i.e. gelatin containing un-freezable water). Glass transition and solids-melting of gelatin at few moisture levels were also reported in the literature [18–22]. Rahman et al. [23] determined the glass transition, unfolding, solids-melting and decomposition temperature of gelatin from different sources at three levels of moisture content. Badii and Howell [24] measured the enthalpy and mechanical relaxation of glassy film of gelatin containing water of 0.08, 0.12 and 0.17 g/g gelatin, respectively.

Most utility of thermal transitions is made in the state diagram which in its simplest form represents the pattern of changes in the phases or states of a material as a function of increasing solids (or moisture content) and temperature [25–27]. Levine and Slade [28] presented state diagram of providone N-vinyl pyrrolidone (PVP) containing glass line, freezing curve, and intersection of these lines as characteristics temperature T_g''. This is most probably the first state diagram in the food science literature. Later they presented another state diagram by glass line, freezing curve, melting line, vapor line, eutectic point, and T_g'' (Levine and Slade [29]). The concept of state diagram was also thoroughly reviewed by Roos and Karel [25] and Roos et al. [30]. The state diagram of date [27,31], mixtures of trehalose, albumin, gelatin, and corn starch [32], rice [33], and spaghetti [34] were presented considering mainly glass line, freezing curve, and maximal-freeze-concentration condition. The ultimate maximal-freeze-concentration is usually defined as the temperature (T_m') when all possible freezable water is transformed into ice and consequently the corresponding solids content is considered as X_s' (i.e. un-freezable water, $X_w' = 1 - X_s'$). The main advantage of drawing a map as state diagram is to help in understanding the complex physical and chemical changes when food's water content and temperature are changed. It also assists in identifying food's stability during storage as well as selecting a suitable condition for processing (i.e. temperature and water content).

Recently, Rahman [8] reviewed the updated form of the state diagram and its applications in foods. The components of the state diagram were also presented. The glass transition temperature, freezing point, end point of freezing, maximal-freeze-concentration condition, solids-melting, vapor line and BET-monolayer line are necessary to develop the proposed sate diagram [8,9]. In the literature a few works are presented for the thermal characteristics required to construct the complete state diagram of gelatin. The objective of this study was to develop the state diagram of bovine gelatin by measuring its glass transition, freezing, unfolding, solids-melting characteristics and ultimate maximal-freeze-concentration conditions by differential scanning calorimetry (DSC). In addition freezing point was also measured by widely accepted cooling curve method.

2. Materials and methods

2.1. Materials

Commercial bovine gelatin was bought from Sigma-Aldrich, Gillingham, Dorset, UK (gelatin powder: catalogue number: G 9382). Moisture content of the bovine gelatin was measured gravimetrically using an oven at 105 °C for at least 18 h of drying.

2.2. Sample equilibration at different water activity

Samples (about 5 g) were stored in air-sealed glass jars (maintained at different relative humidity environment) with a beaker containing saturated salt solutions maintaining a layer of salt crystals at the bottom. A 5 ml beaker containing thymol was also placed inside the jars of higher water activity to prevent mold growth during storage. The temperature of equilibration and duration were 20 °C and 4 weeks, respectively. The salts used to prepare solution for maintaining relative humidity were: $LiCl_2$, CH_3COOK, $MgCl_2$, K_2CO_3, $Mg(NO_3)_2$, NaBr and $SrCl_2$. The water activity of the samples were varied from 0.113 (X_w: 0.049 g/g gelatin) to 0.877 (X_w: 0.209 g/g gelatin) using constant relative humidity environments as mentioned above. Samples containing lower moisture contents were prepared by drying the bovine gelatin in a convection oven at 105 °C (i.e. sample containing moisture below 0.049 g/g sample). Samples at moisture contents 0.13, 0.16, and 0.19 g/g sample were prepared by placing it in airtight jars with beakers containing distilled water. The samples were kept inside until it reached to a predetermined weight and then the samples were stored in an airtight glass bottle at 4 °C for at least 2 days in order to reach uniform moisture distribution. Samples containing higher moisture content (X_w: 0.25–0.90 g/g sample) were prepared by adding predetermined distilled water with thorough mixing with a spatula. The samples were then stored in airtight glass bottles at 4 °C for at least 2 days for achieving uniform moisture distribution. All equilibrated, dried, water mixed samples at different moisture contents were stored at −20 °C until used for DSC measurement or freezing point by cooling curve method.

2.3. Differential scanning calorimetry (DSC)

The freezing, unfolding, glass transition, solids-melting, and decomposition temperatures of gelatin samples at different moisture content were measured by differential scanning calorimetry (DSC Q10, TA Instruments, New Castle, DE, USA). Mechanical refrigerated cooling system was used to cool the sample up to −90 °C. The instrument was calibrated for heat flow and temperature using distilled water (m.p. 0 °C; ΔH_m 334 J/g), and indium (m.p. 156.5 °C; ΔH_m 28.5 J/g). Aluminum pan of 30 ml, which could be sealed with lid were used in all experiments with an empty sealed pan as reference. Nitrogen at a flow rate of 50 ml/min was used as a carrier gas.

2.4. Thermal analysis of samples containing un-freezable water

Samples (containing un-freezable water, X_w: 0.0–0.209 g/g sample) of 10 mg placed in a sealed aluminum pan were cooled to −90 °C at 5 °C/min, and kept for 10 min. It was then scanned from −90 to 350 or 250 °C at a rate of 10 °C/min. The glass transition (a shift in the thermogram line), thermal unfolding (endothermic peak after glass transition), solids-melting (endothermic peak after unfolding), and decomposition (exothermic and endothermic peaks) characteristics were identified from the thermogram. Glass transition was analyzed for the onset, mid, end points of the shift in the thermogram line including change in specific heat during the shift. Thermal unfolding and melting peaks were characterized from initial, maximum slope and peak points and enthalpy involved

in the transitions. Average and standard deviation of 3–6 replicates were obtained for each experiment. Similarly thermogram line with glass transition, thermal unfolding, and solids-melting was also measured for egg albumin and gelatin mixture [24], and gelatin [17–19,21,23]. However, it was identified earlier that ability to trace thermal unfolding in the therogram depended on the types of gelatin as well as their moisture contents [21–23]. In some instances the glass transition shift was merged with the thermal unfolding or solids-melting endotherm when thermal unfolding was absent [17,21–24]. In this situation when it was difficult to trace the glass transition or it is merged with the endotherm, then a second scan was performed after an initial scan above the solids-melting, followed by cooling below the glass transition and then heating again. In this type of protocol a clear glass transition can be traced [17,21,22,35]. However, this approach was unable to maintain the original structure of the sample when second heating scan was used to trace the glass transition [18]. For this reason, in this work glass transition was determined only from the first scan.

2.5. Thermal analysis of samples containing freezable water

A different procedure was used for high water content samples with freezable water (X_w^o: 0.25–0.90 g/g gelatin). First it was identified that sample containing total water 0.25 g/g gelatin or above showed endothermic peak for ice melting during heating. Sample of 10 mg of bovine gelatin powder (X_w^o: 0.25 g/g sample) placed in a sealed aluminum pan were cooled to −90 °C at 5 °C/min, and kept for 10 min. The sample was then scanned from −90 °C at 10 °C/min to 100 °C in order to determine freezing point and *apparent maximal-freeze-concentration* condition [$(T'_m)_a$ and $(T'''_g)_a$]. After knowing the apparent $(T'_m)_a$ and $(T'''_g)_a$, other samples were scanned similarly with 30 min annealing at $[(T'_m)_a - 1]$ °C and then *annealed maximal-freeze-concentration* $(T'_m)_n$ and $(T'''_g)_n$ were determined. The use of annealing condition allowed to maximize the formation of ice before second heating cycle and to avoid the appearance of exothermic or endothermic peak before the glass transition. Similar annealing condition was used by Bai et al. [36] for apple sample. Samples with other moisture contents were also annealed at same conditions as mentioned above. The *ultimate maximal-freeze-concentration* conditions were determined as follows: first the average values of the $(T'_m)_n$ and $(T'''_g)_n$ was determined when these values showed nearly constant at low moisture contents, and the average values were defined as $(T'_m)_u$ and $(T''_g)_u$. The value of maximal-freeze-concentration (X'_s) was determined from the intersection point of the extended freezing curve (T_{FM} versus X_s) by maintaining the similar curvature and drawing a horizontal line passing through ultimate $(T'_m)_u$. Finally X'_s was read on the x-axis by drawing a vertical line passing through the intersection point as mentioned above. The freezing endotherm was characterized by onset, maximum slope, peak, and enthalpy for melting of ice during heating. The initial or equilibrium freezing point was considered as the maximum slope in the ice melting endotherm as suggested by Rahman [27]. The latent heat of fusion of ice was determined by calculating the area of the ice melting endotherm. Similarly the characteristics of unfolding, and solids-melting endotherm were determined.

2.6. Cooling curve method

Initial freezing point (T_{FI}) of gelatin solution at different moisture contents was also measured by the cooling curve method [37]. The gelatin samples of different water content were filled into steel cylinders (2.2 cm internal diameter, 4.5 cm height, 1 mm wall thickness), insulated with polystyrene foam at the top and bottom to allow one dimensional heat transfer, i.e. heat conduction in radial direction only. K-type thermocouples were placed at the geometric center of the cylinder in order to monitor its temperature. The steel cylinder containing gelatin was then placed in a chest freezer maintained at −55 °C and the temperature change was recorded with time. The freezing characteristics were determined from the cooling curve (i.e. temperature *versus* time plot). The initial freezing point was determined from the procedure proposed by Rahman et al. [38]. At the onset of ice formation, a sudden rise in temperature was noticed due to the liberation of heat of fusion, and this assisted in detecting the initial freezing point. The initial or equilibrium freezing point was considered as the highest temperature after the nucleation of ice.

2.7. Theoretical approach

The theoretical Clausius-Clapeyron equation was first used to estimate the freezing point of bovine gelatin, and the equation can be written as:

$$\delta = -\frac{\beta}{\lambda_w} \ln\left[\frac{1 - X_s^o}{1 - X_s^o + EX_s^o}\right] \quad (1)$$

where δ is the freezing point depression ($T_w - T_{FM}$), T_{FM} is the freezing point of food (°C), T_w is the freezing point of water (°C), β is the molar freezing point constant of water (1860 kg K/kg mol), λ_w is the molecular weight of water, X_s^o is the initial solids mass fraction before freezing (g/g sample), and E is the molecular weight ratio of water and solids (λ_w/λ_s). The model parameter E was estimated using SAS non-linear regression [39].

The Clausius-Clapeyron equation is limited to the ideal solution (i.e. for a very dilute solution). Theoretical models can be improved by introducing parameters for non-ideal behavior when fraction of total water is unavailable for the formation of ice. The unfrozen water content B can be defined as the ratio of unfrozen water to the total solids. Chen [40] extended the Clausius-Clapeyron (Eq. (1)) by introducing a parameter B as:

$$\delta = -\frac{\beta}{\lambda_w} \ln\left[\frac{1 - X_s^o - BX_s^o}{1 - X_s^o - BX_s^o + EX_s^o}\right] \quad (2)$$

The model parameters E and B were estimated using SAS non-linear regression. The influence of water content on glass transition temperature is commonly modeled by Gordon-Taylor equation [41]:

$$T_{gm} = \frac{X_s T_{gs} + kX_w T_{gw}}{X_s + kX_w} \quad (3)$$

where T_{gm}, T_{gs} and T_{gw} are the glass transition temperature of mixture, dry solids, and water; X_w and X_s are the mass fraction of water and dry solids (wet basis, g/g sample), and k is the Gordon-Taylor parameter, respectively.

The melting point (loss of crystal state) of a polymer in diluent can be predicted by equation proposed by Flory [42] as:

$$\frac{1}{T_{mi}} - \frac{1}{T_{mi}^s} = \left(\frac{R}{\Delta H_u}\right)\left(\frac{V_u}{V_w}\right)(\varepsilon_w - \chi\varepsilon_w^2) \quad (4)$$

where T_{mi} and T_{mi}^s are the onset of melting temperature for the polymer in the diluent, and pure polymer (i.e. solids) (K), R is the gas constant (8.314 kJ/kg mol K), ΔH_u is the heat of fusion for repeated polymer units in the diluent (kJ/kg), V_w is the molar volume of the diluent (m^3/g mol), ε_w is the volume fraction of the diluent, and χ is the Flory interaction parameter, respectively. This equation has been applied to the melting of starch as a polymer with water as a diluent [43–46]. The volume fraction of water was calculated as (Rahman [65]):

$$\varepsilon_w = \frac{X_w/\rho_w}{X_w/\rho_w + X_p/\rho_s} \quad (5)$$

The density values of water and gelatin (considered as protein) as a function of temperature were estimated from the correlations developed by Choi and Okos [47], and T^s_{mi} was considered as 508 K (i.e. 235 °C).

Various methods have been used to predict the un-freezable water content (X'_w) at the maximal-freeze-concentration condition. The method proposed by Levine and Slade [28] was based on the determination of ΔH_m for a solution at solids content at 0.20 g/g solution, which provided a fast method to determine approximately the un-freezable water content. The un-freezable water can be calculated from the following equation as:

$$X'_w = X^o_w - \frac{(\Delta H_m)_{sample}}{(\Delta H_m)_{water}} \quad (6)$$

where $(\Delta H_m)_{sample}$ is the enthalpy change during melting of ice in the sample, and $(\Delta H_m)_{water}$ is the latent heat of melting of ice considered as 334 kJ/kg. Alternatively $(\Delta H_m)_{sample}$ with the moisture content, and un-freezable water content was calculated from the linear relationship extending to zero values of $(\Delta H_m)_{sample}$ [48].

3. Results and discussion

3.1. Sample containing un-freezable water

The moisture content of the commercial bovine gelatin was determined as 0.097 g/g gelatin. Fig. 1A shows DSC thermogram of the sample containing un-freezable water (moisture: 0.036 g/g gelatin) within the temperature range 0–350 °C. This thermogram indicates glass transition (shift in thermogram line, marked as 'A'), thermal unfolding (endothermic peak, marked as 'B'), solids-melting (endothermic peak, marked as 'S'), and decomposition (exothermic and endothermic peaks, marked as 'D' and 'E'), respectively (Fig. 1A). All other samples were performed within the range 0–250 °C in order to identify glass transition, thermal unfolding and solids-melting (Fig. 1B). The glass transition was identified as onset, peak and end of the shift (marked as 'A') in the thermogram line, and endothermic peak as identified B (thermal unfolding) and S (solids-melting) was characterized as peak (marked as 'p'), maximum slope (marked as 'm'), extended line of maximum slope to the base of thermogram line (marked as 'i'), and end of peak (marked as 'e'). In the cases of bovine gelatin only one melting endothermic peak was observed. However, wheat and potato starch showed single and multiple melting endothermic peak(s) with varying nature of sharp or wide. The shape of the melting peak depended on the moisture content in the sample [49–51]. This suggested the presence of different levels or types of organized structure in the starch granules. The thermal unfolding, glass transition and melting temperature decreased with the decrease of solids content up to 0.85 g/g gelatin, and then remained constant with further decrease in solids content (i.e. increase of water content) (Table 1). Similar result for denaturation of protein was also reported by D'Cruzand and Bell [17]. The difference between glass transition and melting temperature remained nearly similar over the solids content, whereas the difference between melting and unfolding temperature was higher at low solids content. As the solids content decreased (i.e. moisture content increased), hydrogen bond disruption associated with the helix-coil transition was easier leading to melting just after unfolding.

The endothermic peak for denaturation was related to the helix-coil transition as described by Marshall and Petrie [19], Sobral et al. [21] and Levine and Slade [52]. The large endothermic peak (i.e. melting) was first discussed by Levine and Slade [52] and hypothesized that this thermal transition represented an intramolecular *trans-cis* isomerization of the polyproline regions of gelatin's peptide backbone, which required energy input. D'Cruzand and Bell [17] scanned gelatin to different temperatures within the peak,

Table 1
Glass transition and melting of bovine gelatin (samples with un-freezable water).

a_w	X_w	Glass transition				Thermal unfolding				Melting of solids				
		T_{gi} (°C)	T_{gp} (°C)	T_{ge} (°C)	ΔC_p (J/kg K)	T_{ui} (°C)	T_{um} (°C)	T_{up} (°C)	ΔH_u (kJ/kg)	T_{mi} (°C)	T_{mm} (°C)	T_{mp} (°C)	T_{me} (°C)	ΔH (kJ/kg)
	0.000	160 (9)	167 (13)	176 (7)	193 (84)	212 (3)	218 (3)	235 (5)	11.0 (2)	235 (2)	261 (2)	276 (3)	283 (3)	49 (8)
–	0.013	121 (18)	142 (24)	166 (8)	433 (192)	162 (10)	178 (8)	193 (11)	0.5 (1)	205 (6)	214 (4)	224 (6)	236 (2)	10 (3)
–	0.017	107 (19)	126 (29)	156 (18)	546 (78)	154 (10)	173 (5)	192 (4)	1.8 (2)	210 (1)	219 (2)	225 (2)	232 (1)	60 (9)
–	0.036	105 (27)	127 (22)	143 (20)	1010 (210)	135	140	150	6.0	180 (16)	204 (20)	212 (20)	231 (15)	50 (7)
0.113	0.049	86 (1)	94 (1)	96 (1)	484 (90)	102 (6)	107 (6)	109 (4)	3.3 (2)	150 (11)	132 (15)	150 (26)	215 (24)	109 (6)
0.216	0.066	78 (4)	87 (2)	90 (3)	435 (60)	103 (2)	105 (1)	114 (6)	2.7 (2)	121 (4)	135 (8)	153 (13)	195 (2)	123 (13)
0.336	0.076	68 (4)	73 (1)	78 (4)	643 (120)	99 (2)	100 (2)	111 (3)	4.1 (2)	102 (14)	113 (8)	127 (4)	204 (3)	184 (32)
0.431	0.088	61 (2)	67 (2)	71 (2)	436 (18)	93 (2)	97 (1)	102 (5)	1.3 (1)	114 (1)	118 (2)	125 (2)	199	147 (18)
0.577	0.096	59 (3)	64 (2)	67 (2)	817 (222)	87 (3)	92 (1)	92 (2)	0.8 (1)	90 (34)	109 (14)	123 (9)	200	220 (34)
0.589	0.108	57 (2)	61 (2)	64 (2)	921 (126)	84 (1)	87 (1)	89 (1)	1.5 (1)	86 (33)	110 (19)	117 (1)	202 (4)	239 (29)
–	0.130	43 (1)	46 (1)	50 (1)	337 (42)	87 (3)	89 (2)	92 (1)	2.2 (1)	97 (4)	111 (2)	123 (2)	197 (4)	231 (35)
–	0.160	35 (2)	39 (1)	43 (2)	460 (155)	77	80	83	1.7	75 (11)	97 (10)	113 (4)	190 (12)	287 (27)
–	0.190	36 (2)	41 (1)	43 (2)	503 (144)	72	76	85	0.6	70 (7)	85 (10)	102 (7)	165 (2)	300 (6)
0.877	0.209	38 (2)	52 (2)	54 (2)	1003 (84)	61 (3)	52 (4)	54 (3)	1.3 (1)	82 (4)	100 (1)	115 (1)	190	425 (26)

Note: DSC heating rate (10 °C/min).

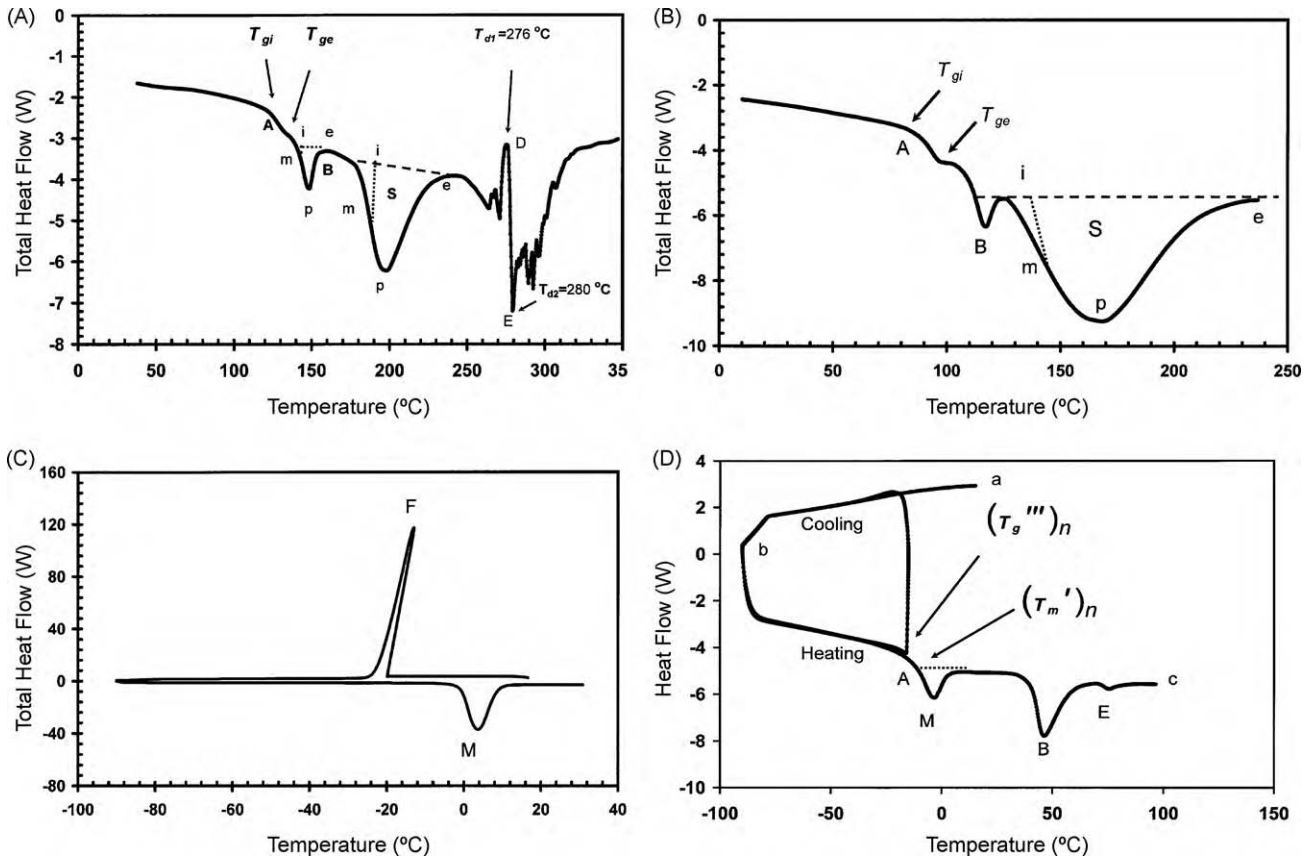

Fig. 1. (A) DSC thermogram of bovine gelatin containing water 0.036 g/g bovine (no freezable water). (B) DSC thermogram of bovine gelatin containing water 0.049 g/g sample (no freezable water). (C) DSC thermogram of sample showing freezing of water during cooling and melting of ice during heating (X_w^o: 0.90 g/g sample). (D) DSC thermogram (with annealing at $[(T'_m)_a - 1]$ for 30 min) of sample showing no freezing of water during cooling; a shift (marked as 'A') in the thermogram line just before melting of ice, a endothermic peak for melting of ice (marked as 'M'), and another endothermic peak for unfolding during heating (marked as 'B'); $(T'_m)_n$ and $(T'''_g)_n$ are the annealed maximal-freeze-concentration condition (X_w^o: 0.25 g/g sample).

and observed different degrees of discoloration immediately after cutting the sample. For example, a sample heated to a temperature immediately after the onset of the large peak was dark yellow, whereas a sample heated to a temperature beyond the peak was dark brown to black. This indicated that isomerization and/or decomposition reactions could occur during the melting process. Marshall and Petrie [19] and Slade and Levine [53] proposed that heating the sample beyond the glass transition caused a disruption of the crystalline (or highly structured) regions and gelatin behaves as a molecularly dispersed melted plastic.

3.2. Sample containing freezable water

Fig. 1C shows cooling and heating (at 10 °C/min) DSC thermograms for gelatin with high moisture content indicating ice forming exotherm (marked as 'F') due to the freezing of water during cooling and ice melting endotherm (marked as 'M') during heating. At low moisture content the freezing exotherm cannot be traced during cooling as shown in Fig. 1D. In the case of sample containing 0.25 g/100 g gelatin, cooling and heating scan was performed without annealing in order to determine apparent maximal-freeze-concentration condition $[(T'_m)_a$ and $(T'''_g)_a]$. The values of $(T'_m)_a$ and $(T'''_g)_a$ were found as −13.5 and −16.5 °C, respectively for sample containing 0.25 g/100 g sample. Fig. 1D shows a typical thermogram with cooling and heating of annealed sample at $T'_m - 1$ for 30 min for achieving annealed maximal-freeze-concentration condition $[(T'''_g)_n$ and $(T'_m)_n]$ at various moisture content. The shift before ice melting endotherm marked as 'M' and following unfolding peak is marked as 'B'. In this case, glass transition can be considered from the shift before ice melting endotherm in the thermogram line as annealed maximal-freeze concentration conditions $[(T'''_g)_n$ and $(T'_m)_n]$ merged with the ice melting endotherm. The values of $(T'''_g)_n$ decreased up to solids content 0.5 g/g gelatin and then it remained nearly constant (Table 2). Similar trend was also observed for $(T'_m)_n$ up to solids content 0.4 g/g gelatin. The ultimate maximal-freeze-concentration conditions was estimated from the average values $(T'''_g)_u$ as −14.9 °C (X_s: 0.5–0.25 g/g gelatin) and $(T'_m)_u$ as −11.9 °C (X_s: 0.4–0.25 g/g gelatin), respectively.

The effect of heating rate on the freezing point and apparent maximal-freeze-concentration condition are also studied in order to determine which heating rate should be used to measure the characteristics of the freezing process. Fig. 2 shows the effect of heating rate on the freezing point (T_{FM}), enthalpy at the ice melting, and apparent maximal-freeze-concentration condition $(T'_m)_a$, and $(T'''_g)_a$. Fig. 2A shows that T_{FM} increased initially, reached to a plateau region within the heating rate 10–30 °C/min and then increased again. The completeness of melting process can be explained from the enthalpy at the ice melting endotherm as shown in Fig. 2B. The plateau region within the heating rate 10–30 °C/min indicated the maximum possible melting of ice. Thus heating process within the 10–30 °C/min should be used to determine the heating (i.e. representation of the freezing) process by DSC method. The effect of heating rate on $(T'_m)_a$ was observed similar to the T_{FM} (Fig. 2C), whereas $(T'''_g)_a$ initially increased exponentially followed by a relatively linear rise after heating rate 10 °C/min (Fig. 2D). In this work the heating rate was used as 10 °C/min, since maximum instantaneous melting of ice was achieved with in the heating rate 10–30 °C/min (Fig. 2B).

Table 2
Glass transition and maximal-freeze concentration conditions of bovine gelatin.

X_w	Melting of ice				Glass transition			Thermal unfolding			
	T_{FC} (°C)	T_{FM} (°C)	T_{FP} (°C)	ΔH_{ice} (kJ/kg)	$(T'_m)_n$ (°C)	$(T'''_g)_n$ (°C)	ΔC_p (J/kg K)	T_{ui} (°C)	T_{um} (°C)	T_{up} (°C)	ΔH_u (kJ/kg)
0.25	−11.0 (3.0)	−9.0 (0.6)	−5.7 (3.5)	7 (2)	−12.7 (1.6)	−15.7 (2.3)	490 (161)	33.8 (1.1)	35.5 (0.9)	54.1 (0.9)	8.0 (2.2)
0.30	−9.7 (0.5)	−7.1 (0.4)	−3.7 (0.4)	17 (4)	−11.7 (1.9)	−14.7 (2.4)	633 (102)	32.9 (1.5)	34.7 (1.5)	61.0 (1.4)	13.2 (1.9)
0.35	−8.7 (0.8)	−5.6 (1.3)	−2.1 (1.3)	36 (8)	−11.3 (1.8)	−13.6 (2.7)	1023 (765)	31.3 (1.6)	32.8 (1.8)	53.6 (1.6)	10.5 (1.1)
0.40	−6.7 (2.7)	−3.5 (2.8)	0.3 (4.9)	62 (15)	−11.7 (4.3)	−14.7 (2.8)	1016 (150)	31.3 (7.6)	35.2 (1.6)	52.7 (8.2)	8.2 (2.6)
0.50[a]	−4.7 (1.0)	−2.7 (0.3)	0.3 (2.0)	108 (21)	−9.7 (1.5)	−15.7 (1.3)	1197 (150)	25.9 (8.8)	29.3 (5.7)	41.7 (4.8)	4.9 (3.3)
0.60	−3.7 (0.2)	−1.8 (0.2)	3.3 (2.6)	177 (17)	−8.7 (0.8)	−10.7 (0.8)	1654 (114)	30.9 (1.8)	32.4 (1.5)	41.8 (0.5)	4.0 (0.5)
0.70	−3.4 (0.2)	−1.2 (0.4)	1.3 (1.0)	208 (12)	−6.7 (0.9)	−6.7 (0.9)	1909 (384)				
0.80	−3.3 (0.3)	−1.1 (0.5)	5.3 (0.8)	241 (13)	−4.7 (0.9)	−5.7 (1.2)	1968 (300)				
0.90[b]	−2.7 (0.4)	−0.2 (0.7)	3.3 (1.6)	248 (11)	−3.7 (1.0)	−5.7 (0.9)	2022 (198)				

Note: DSC heating rate: 10 °C/min.
[a] $T_{FI} = -3.2 \pm 0.87$ °C (cooling curve method).
[b] $T_{FI} = -0.33 \pm 0.06$ °C (cooling curve method).

The value of E was estimated as 0.029 from Eq. (1), and the effective molecular weight of gelatin solids was estimated as 614. The reported values of E were found to be 0.147 for dates [27], 0.238 for apples [36], 0.068 for garlic [54], 0.082 for squid [55], and 0.071 for tuna meat [38], respectively. Interestingly it could be seen that sugar based product showed higher values of E (i.e. low molecular weight) compared to non-sugar carbohydrate and protein based food product.

The model parameters E and B of Eq. (2) were estimated using SAS non-linear regression and found to be 0.026 and 0.050 g/g dry solids (in wet basis, unfrozen water, $X'_w = 0.048$; and solids content, $X'_s = 1 - 0.048 = 0.952$), respectively. The mean square error from experimental data using Eqs. (1) and (2) were 0.14 and 0.12, respectively. This indicates that more accurate prediction can be done using Eq. (2). The reported values of E and B were found to be 0.129 and 0.053 for dates [27], 0.080 and −0.062 for garlic [54], 0.012 and 0.329 for rice [33], 0.033 and 0.383 for tuna [38], 0.027 and 0.303 for king fish [56], 0.067 and 0.120 for squid, 0.041 [55], 0.041 and 0.650 for fresh seafood [55], respectively. However X'_w estimated from B was found to be 0.048 g/g gelatin, which was relatively very low compared to the other methods (as discussed later) although mathematical accuracy in prediction of freezing point could be achieved. When parameters are estimated by non-linear regression using experimental data, Eq. (2) is transformed to the empirical nature although it is based on the physics. This is one of the generic problems when theoretical-based model is extended to fit the experimental data [27].

3.3. State diagram

Fig. 3A shows the freezing point (maximum slope of heat flow, and initial freezing point from cooling curve) and annealed maximal-freeze-concentration condition [$(T'''_g)_n$ and $(T'_m)_n$] as a function of solids content. The freezing curve as ef represents the

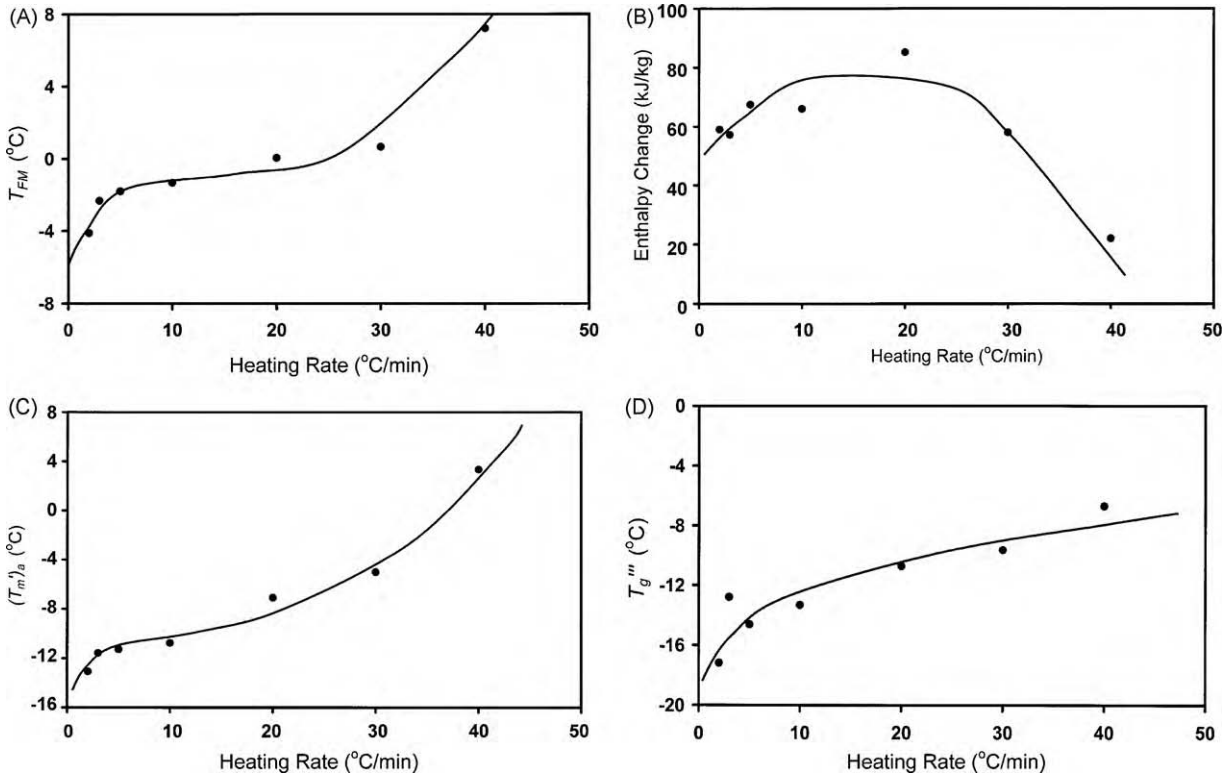

Fig. 2. (A) The plot of T_{FM} as a function of heating rate for gelatin containing moisture 0.60 g/g sample. (B) The plot of melting enthalpy of ice as a function of heating rate for gelatin containing moisture 0.60 g/g sample. (C) Plot of $(T'_m)_a$ as a function of heating rate for gelatin containing moisture 0.60 g/100 g sample. (D) Change of $(T'''_g)_a$ as a function of heating rate for gelatin containing moisture 0.60 g/g sample.

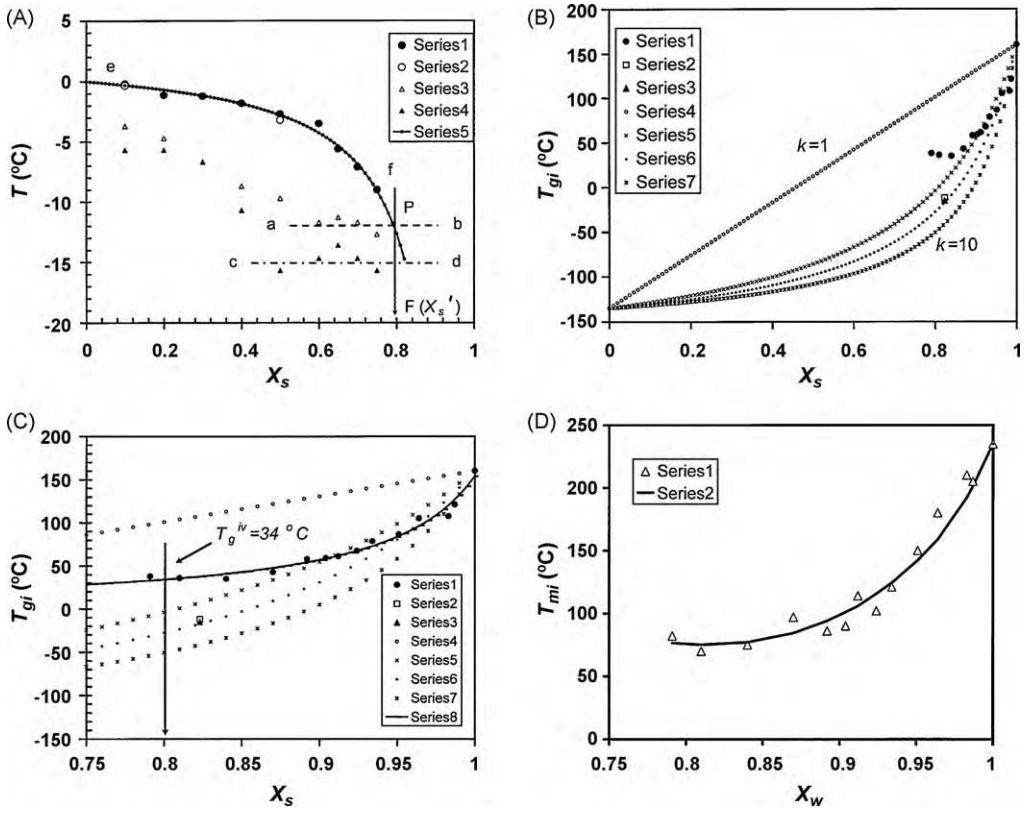

Fig. 3. (A) State diagram showing freezing curve, annealed and ultimate maximal-freeze concentration conditions; ef: freezing curve, ab: ultimate T'_m, cd: ultimate T'''_g, F: X'_s, series 1: freezing point measured by DSC method, series 2: initial or equilibrium freezing point measured by cooling curve method, series 3: annealed T'_m, series 4: annealed T'''_g, series 5: prediction model based on Eq. (2). (B) Experimental onset of glass transition temperature and Gordon-Taylor model equation for $k = 1$, 5, 7 and 10, series 1: experimental values, series 2: T'_m, series 3: T'''_g, series 4: $k = 1$, series 5: $k = 5$, series 6: $k = 7$, series 7: $k = 10$. (C) Experimental onset of glass transition temperature, original Gordon-Taylor model equations (Eq. (3), for $k = 1$, 5, 7 and 10) and modified (Eq. (7)), series 1: experimental values, series 2: T'_m, series 3: T'''_g, series 4: $k = 1$, series 5: $k = 5$, series 6: $k = 7$, series 7: $k = 10$, series 8: modified Gordon-Taylor model (Eq. (7)). (D) Experimental onset of solids-melting temperature and Flory model equation, series 1: experimental values, series 2: Flory's equation.

formation of ice from solution and it has a negative gradient showing the expected decrease in the freezing point with increasing concentration of solids. The procedure to determine X'_s for the ultimate maximal-freeze-concentration is shown in Fig. 3A. The value of X'_s was determined from the intersection (point 'P' in Fig. 3A) of the extended freezing curve ef by maintaining the similar curvature (theoretical prediction model, Eq. (2)) and a horizontal line (ab) passing thorough $(T'_m)_u = -11.9\,^\circ$C (as point 'P' in Fig. 3A). Finally X'_s was read, on the x-axis by drawing a vertical line passing through point 'P', as 0.80 g/g gelatin. The un-freezeable water content can be estimated as ($X'_w = 1 - X'_s$) and the water in the right side of the vertical line PF in Fig. 3A did not show any freezable water (i.e. unable to form ice even at very low temperature). Thus, un-freezable water determined from state diagram was found to be 0.20 g/g gelatin.

The Gordon-Taylor model based on Eq. (3) is plotted in Fig. 3B for different values of k as 1, 5, 7, and 10 with the experimental onset of glass transition temperature of gelatin. At low moisture content glass transition decreased with the increase of solution water content due to plasticization, whereas at or above 0.16 g/g gelatin moisture content (i.e. 0.84 g/g gelatin) glass transition showed nearly constant values (Table 2). In the case of starch, Biliaderis et al. [50] observed fully plasticization at moisture content 0.30 g/g starch and above this level glass transition showed constant value. They proposed that above this moisture level (i.e. maximum plasticization occurred) water formed a separate pure solvent water phase outside the starch granules. It is clear in Fig. 3B that the data points could not be modeled by Gordon-Taylor model when the data at low moisture deviate from the Gordon-Taylor line. In this case, Rahman [9] proposed modified Gordon-Taylor model as:

$$T_{gm} = \frac{X_s T_{gs} + k_c X_w T_c}{X_s + k_c X_w} \tag{7}$$

In the above equation T_c is considered as critical temperature and it is related to T_g^{iv} as defined by Rahman [9]. The values of T_g^{iv} was determined from the intersection point of the glass transition line and a vertical line through $X'_s = 0.80$. From Fig. 3C, T_g^{iv} was found as 34.0 °C. In the case of starch the value of T_g^{iv} can be estimated as 68.0 °C and X'_s as 0.70 g/g starch using the data of Biliaderis et al. [50]. In comparison to the Eq. (3), the value of T_c can be related as:

$$T_c = T_g^{iv}(1 - X'_s) \tag{8}$$

This correction was needed since origin of Gordon-Taylor equation is now shifted from 0 to X'_s. The value of T_c was estimated as 6.8 °C from the above Eq. (8). The modified Gordon-Taylor model parameters T_{gs} and k_c were estimated as 153.7 °C and 17.3, respectively using SAS [39] non-linear regression procedure. The experimental data and model equation are shown in Fig. 3C. The glass transition of the dry gelatin as 153.7 °C was lower side of the reported literature values 155–200 °C as compiled by D'Cruzand and Bell [17]. This variation was due to the differences in source, molecular weight, and preparation.

3.4. Solids-melting point

The values of ($RV_u/\Delta H_u V_w$) and χ based on Eq. (4) were estimated as 7.77×10^{-3} and 2.15 using SAS [39] non-linear regression.

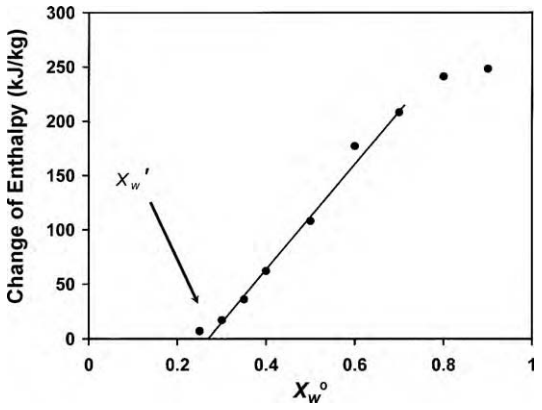

Fig. 4. Change of enthalpy for ice melting as a function of total water content.

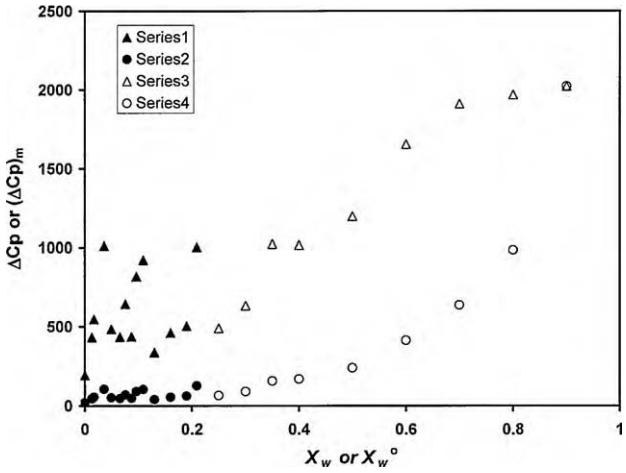

Fig. 5. Change of specific heat as a function of total water at the glass transition temperature: series 1: ΔC_p below freezing, series 2: $(\Delta C_p)_m$ below freezing, series 3: ΔC_p above freezing, $(\Delta C_p)_m$ above freezing.

The experimental values and predicted line from Flory equation are shown in Fig. 3D. In general these parameters were not usually reported in the literature, instead linear relationship between $(1/T_{mi})$ *versus* ε_w were presented assuming χ equal to zero [45,46,49–51]. In the case of gelatin, χ showed much higher value compared to zero as assumed for starch by others.

3.5. Un-freezable water from different methods

The $(\Delta H_m)_{sample}$ is the enthalpy change during melting of ice in the sample as shown in Table 2 and plotted with the moisture content, and un-freezable water content was calculated from the linear relationship extending to zero values of $(\Delta H_m)_{sample}$ (Fig. 4). Alternatively a linear regression for bovine gelatin can be developed as:

$$(\Delta H_m)_{sample} = 479.2X_w^o - 124.3 \quad (9)$$

The values of X_w' can be estimated from the above Eq. (9) as 0.26 when $(\Delta H_m)_{sample}$ is equal to zero. Using graphical plot, the X_w' for gelatinized wheat starch [57], cellulose [15], gluten [58] were observed as 0.30, 0.16, 0.18 g/g sample, respectively. The procedure by Eqs. (6) and (9) could give error due to two reasons [59]: (i) enthalpy of pure water (heat of fusion) is a function of temperature and this can give error up to 10% if freezing point depression is 5–10 °C, (ii) heat represented by the area under the curve is a combination of heat of fusion of ice plus sensible heat taken by freshly melted water. The un-freezable water estimated from the ice melting endotherm (based on Eq. (6)) decreased from 0.23 to 0.07 with the increasing initial water concentration. Similar variation was also observed in the cases of fructose [60], sucrose [61], and date [27]. The average value was estimated as 0.17 g/g gelatin ± 0.07.

The un-freezable water content (0.048 g/g gelatin) from freezing point prediction model (Eq. (2)) is not a reliable method although it gives accurate prediction for freezing point. It was not recommended for a number of reasons [27,54]. In many instances the values of B were found to be very low or even negative. The negative value of B indicated that a fraction of solids behave as solvent. This explanation may not be an accepted argument. Chen [40] indicated that freezing point depression is caused by the complex interaction between solutes and water and it can be the equivalent increase in free water. Thus, values of B can either be positive or negative depending on the behavior of freezing point data. In case of numbers of solutes, they found negative values of B. In addition, the un-freezable water content measured by enthalpy and state diagram do not relate with the values determined by this method. For this reason, Rahman [27] indicated that although Eq. (2) can predict the freezing point with accuracy, this does not explain the physics when experimental data on freezing point are fitted to the equation (although it was originally based on the physics) [54]. The reasons could be: (i) when the parameters are estimated by non-linear regression, different local optimized regions could be found based on the initial values used in the optimization. However, this is one of the generic problems that exist when a theoretical-based model with more than two parameters is used to fit the experimental data [62,63]. (ii) In addition, when data are fitted by regression, they provided the mathematical relation rather physics. The accuracy of Eq. (2) was also demonstrated by Rahman [64] and Rahman and Driscoll [55] without extensive evidence that its parameters represent real physical meaning.

Ablett et al. [60] mentioned that calculation of un-freezable water by extending freezing line to glass temperature curve should be most reliable method. This was further confirmed by Rahman [27] and Rahman et al. [54]. It is therefore recommended that the determination of un-freezable water is most acceptable and accurate when T_m' in the state diagram is used since this is the real point when all possible freezable water formed ice and it was experimentally evident by achieving ultimate maximal-freeze-concentration condition, which could be achieved with slow cooling and annealing (i.e. holding the sample at a specific temperature for predetermined duration).

3.6. Specific heat change at the glass transition

Fig. 5 shows the change of specific heat at the glass transition for the bovine gelatin containing freezable and un-freezable water content. The change in specific heat for the bovine gelatin was found to be random at low moisture content and average value was estimated as 587 ± 255 J/kg K (based on total sample mass). The high random variability indicated the existence of greater heterogeneity in the material. Similarly Rahman et al. [23] did not found any trend in the specific heat change for the different types of gelatin containing only un-freezable water. Fig. 5 also shows that specific heat change increased with the increase of water content and remained constant at higher water content. Higher changes indicated the increase of amorphous component in the bovine gelatin. Fig. 5 also shows the modified $(\Delta C_p)_m$ based on dry solids basis. The values of $(\Delta C_p)_m$ was estimated as [65]:

$$(\Delta C_p)_m = \Delta C_p \left(\frac{1 - X_w}{1 - X_w^o}\right) \quad (10)$$

where X_w^o is the highest moisture content in this study and the modification was based on the total solids basis at that moisture

content. In the literature there are little works available for the specific heat change at the glass transition for different types of foods. This characteristic could be used to explore the molecular behavior of the gelatin as a function of water content.

4. Conclusion

Commercial gelatin at initial moisture content of 0.097 g/g sample was prepared at different moisture levels by equilibrating it at different relative humidity values, drying or adding predetermined water in it. Thermal characteristics (freezing point, glass transition, unfolding temperature, solids-melting temperature and maximal-freeze-concentration condition) were measured by DSC in order to develop its state diagram. The glass transition, unfolding, and solids-melting decreased with the decrease of solids up to solids content 0.84 g/g gelatin and then remained constant. The difference between glass transition and melting temperature remained nearly similar over the solids content, whereas the difference between melting and unfolding temperature was higher at low solids content. In the case of bovine gelatin, ultimate $(T'_m)_u$ and $(T'''_g)_u$ were found as −11.9 and −14.9 °C, respectively. The un-freezable water content was found as 0.20 g/g gelatin. The developed state diagram of commercial bovine gelatin can be used in determining its structural functionality as a function of temperature and moisture content.

Acknowledgement

The authors would like to acknowledge the support of Sultan Qaboos University towards this research in developing fish skin gelatin.

References

[1] P.J. Flory, E.S. Weaver, J. Am. Chem. Soc. 82 (1960) 4518–4525.
[2] R. Hinterwaldner, Technology of gelatin manufacture, in: A.G. Ward, A. Courts (Eds.), The Science and Technology of Gelatin, Academic Press, London, UK, 1977, pp. 315–364.
[3] J.D. Ferry, Macromolecules 24 (1991) (1991) 5237–5245.
[4] G.W. White, S.H. Cakebread, J. Food Technol. 1 (1966) 73–82.
[5] B. Luyet, D. Rasmussen, Biodynamica 10 (1968) 167–191.
[6] Y.H. Roos, Phase transitions and transformations in food systems, in: R. Heldman, D.B. Lund (Eds.), Handbook of Food Engineering, Marcel Dekker, New York, 1992, pp. 145–197.
[7] Y. Roos, J. Food Eng. 24 (1995) 339–360.
[8] M.S. Rahman, Trends Food Sci. Technol. 17 (2006) 129–141.
[9] M.S. Rahman, Int. J. Food Properties 12 (2009) 726–740.
[10] Y. Liu, B. Bhandari, W. Zhou, J. Agric. Food Chem. 54 (2006) 5701–5717.
[11] R.B. Duckworth, Solute mobility in relation to water content and water activity, in: L.B. Rockland, G.F. Stewart (Eds.), Water Activity: Influences on Food Quality, Academic Press, New York, 1981, pp. 295–317.
[12] J. Perez, J. Food Eng. 22 (1994) 89–114.
[13] S.J. Richardson, M.P. Steinberg, Applications of nuclear magnetic resonance, in: L.B. Rockland, L.R. Beuchat (Eds.), Water Activity: Theory and Applications to Food, Marcel Dekker, New York, 1987.
[14] L. Slade, H. Levine, A food polymer science approach to structure property relationships in aqueous food systems: non-equilibrium behavior of carbohydrate-water systems, in: H. Levine, L. Slade (Eds.), Water Relationships in Food, Plenum Press, New York, 1991, pp. 29–101.
[15] E. Vittadini, L.C. Dickinson, P. Chinachoti, Carbohydr. Polym. 46 (2001) 49–57.
[16] L.N. Bell, M.J. Hageman, J.M. Bauer, Biopolymers 35 (1995) 201–209.
[17] N.M. D'Cruzand, L.N. Bell, J. Food Sci. 70 (2005) E64–E68.
[18] L. Bell, D.E. Touma, J. Food Sci. 61 (1996) 807–828.
[19] A.S. Marshall, S.E.B. Petrie, J. Photogr. Sci. 28 (1980) 128–134.
[20] S.S. Sablani, S. Kasapis, Y. Al-Rahbi, M. Al-Mugheiry, Drying Technol. 20 (2002) 2081–2092.
[21] P.J.A. Sobral, A.M.Q.B. Habitante, Food Hydrocolloids 15 (2001) (2001) 377–382.
[22] F.M. Vanin, P.J.A. Sobral, F.C. Menegalli, R.A. Carvalho, A.M.Q. Habitante, Food Hydrocolloids 19 (2005) 899–907.
[23] M.S. Rahman, G.S. Al-Saidi, N. Guizani, Food Chem. 108 (2008) (2008) 472–481.
[24] F. Badii, N.K. Howell, Food Hydrocolloids 20 (2006) (2006) 630–640.
[25] Y.H. Roos, M. Karel, Food Technol. 45 (1991) 66–71.
[26] Y.H. Roos, Water activity and physical state effects on amorphous food stability, J. Food Process. Preserv. 16 (1993) 433–447.
[27] M.S. Rahman, Int. J. Food Properties 7 (2004) 407–428.
[28] H. Levine, L. Slade, Carbohydr. Polym. 6 (1986) 213–244.
[29] H. Levine, L. Slade, The glassy state in applications for the food industry, with an emphasis on cookie and cracker production, in: J.M.V. Blanshard, P.J. Lillford (Eds.), The Science and Technology of the Glassy State in Foods, University of Nottingham Press, Nottingham, 1993.
[30] Y.H. Roos, M. Karel, J.L. Kokini, Food Technol. 50 (1996) 95–108.
[31] N. Guizani, G.S. Al-Saidi, M.S. Rahman, S. Bornaz, A.A. Al-Alawi, J. Food Eng. 99 (2010) 92–97.
[32] K.J. Singh, Y.H. Roos, Food Sci. Technol. 39 (2006) 930–938.
[33] S.S. Sablani, L. Bruno, S. Kasapis, R.M. Symaladevi, J. Food Eng. 90 (2009) 110–118.
[34] M.S. Rahman, W. Senadeera, A. Al-Alawi, T. Truong, B. Bhandari, G. Al-Saidi, Food Bioprocess Technol., in press, doi:10.1007/s11947-009-0258-z.
[35] M. Iijima, K. Nakamura, T. Hatakeyama, H. Hatakeyama, Carbohydr. Polym. 41 (2000) 101–106.
[36] Y. Bai, M.S. Rahman, C.O. Perera, B. Smith, L.D. Melton, Food Res. Int. 34 (2001) 89–95.
[37] M.S. Rahman, N. Guizani, M. Al-Khaseibi, S. Al-Hinai, S.S. Al-Maskri, K. Al-Hamhami, Food Hydrocolloids 16 (2002) 653–659.
[38] M.S. Rahman, S. Kasapis, N. Guizani, O. Al-Amri, J. Food Eng. 57 (2003) 321–326.
[39] SAS, The SAS System for Windows, Version 8.02, SAS Institute, Carry, NC, 2001.
[40] C.S. Chen, J. Food Sci. 51 (1986) 1537–1553.
[41] M. Gordon, J.S. Taylor, J. Appl. Chem. 2 (1952) 493–500.
[42] D.J. Flory, Principles of Polymer Chemistry, Cornell University Press, Ithaca, NY, 1953.
[43] J.W. Donovan, Biopolymers 18 (1979) 263–275.
[44] C.G. Biliaderis, T.J. Maurice, J.R. Vose, J. Food Sci. 45 (1980) (1980) 1669–1674.
[45] F. Nakazawa, J. Takahashi, M. Takada, Biosci. Biotechnol. Biochem. 62 (1998) 248–252.
[46] J. Lelievre, Starch gelatinization, J. Appl. Polym. Sci. 18 (1973) 293–296.
[47] Y. Choi, M.R. Okos, Effects of temperature and composition on thermal properties of foods, in: M. LeMaguer, P. Jelen (Eds.), Food Engineering and Process Applications: vol. 1. Transport Phenomena, Elsevier Applied Science, London, 1986, pp. 93–101.
[48] D. Simatos, M. Faure, E. Bonjour, M. Couach, Cryobiology 12 (1975) 202–208.
[49] J.W. Donovan, K. Lorenz, K. Kulp, Cereal Chem. 60 (1983) 381–387.
[50] C.G. Biliaderis, C.M. Page, T.J. Maurice, B.O. Juliano, J. Agric. Food Chem. 34 (1986) 6–14.
[51] J.K. Jang, Y.R. Pyun, Starch 48 (1996) 48–51.
[52] H. Levine, L. Slade, Water as a plasticizer: physico-chemical aspects of low-moisture polymeric systems, in: F. Franks (Ed.), Eater Science Reviews, vol. 3, Cambridge University Press, Cambridge, 1988, pp. 79–185.
[53] L. Slade, H. Levine, Polymer-chemical properties of gelatin in foods, in: A.M. Pearson, T.R. Dutson, A.J. Balley (Eds.), Advances in Meat Research: Collagen as a Food, AVI, New York, 1987, pp. 251–266.
[54] M.S. Rahman, S.S. Sablani, N. Al-Habsi, S. Al-Maskri, R. Al-Belushi, J. Food Sci. 70 (2005) E135–E141.
[55] M.S. Rahman, R.H. Driscoll, Int. J. Food Sci. Technol. 29 (1994) 51–61.
[56] S.S. Sablani, M.S. Rahman, S. Al-Busaidi, N. Guizani, N. Al-Habsi, R. Al-Belushi, B. Soussi, Thermochim. Acta 462 (2007) 56–63.
[57] Y. Vodovotz, P. Chinachoti, Food Sci. 61 (1996) 932–941.
[58] G. Cherian, P. Chinachoti, Cereal Chem. 73 (1996) 618–624.
[59] T.W. Schenz, B. Israel, M.A. Rosolen, Thermal analysis of water-containing systems, in: H. Levine, L. Slade (Eds.), Water Relationships in Food, Plenum Press, New York, 1991.
[60] S. Ablett, M.J. Izzard, P.J. Lillford, I. Arvanitoyannis, M. Blanshard, Carbohydr. Res. 246 (1993) 13–22.
[61] Y. Roos, M. Karel, Int. J. Food Sci. Technol. 26 (1991) 553–566.
[62] M.S. Rahman, Drying Technol. 23 (2005) 695–715.
[63] M.S. Rahman, R.H. Al-Belushi, Int. J. Food Properties 9 (2006) 421–437.
[64] M.S. Rahman, J. Food Eng. 21 (1994) 127–136.
[65] M.S. Rahman, Int. J. Food Properties 6 (2003) 61–72.